forests

MDPI

Article

Contrasts in Top Soil Infiltration Processes for Degraded vs. Restored Lands. A Case Study at the Perijá Range in Colombia

Sergio Esteban Lozano-Baez [1,*], Yamileth Domínguez-Haydar [1], Bob W. Zwartendijk [2,3], Miguel Cooper [4], Conrado Tobón [5] and Simone Di Prima [6]

[1] Department of Biology, Universidad del Atlántico, Carrera 30 Número 8-49, Puerto Colombia 081001, Colombia; yamilethdominguez@mail.uniatlantico.edu.co
[2] Research and Innovation Centre Techniek, Ontwerpen en Informatica, Inholland University of Applied Sciences, Bergerweg 200, 1817 MN Alkmaar, The Netherlands; Bob.Zwartendijk@inholland.nl
[3] Hydrology and Quantitative Water Management Group, Wageningen University & Research, 6700 HB Wageningen, The Netherlands
[4] Luiz de Queiroz School of Agriculture, University of São Paulo, Av. Pádua Dias 11, Piracicaba 13418-900, Brazil; mcooper@usp.br
[5] Department of Forestry and Environmental Conservation, Universidad Nacional de Colombia, Carrera 65 59A-110, Medellín 050023, Colombia; ctobonm@unal.edu.co
[6] Agricultural Department, University of Sassari, Viale Italia, 39, 07100 Sassari, Italy; sdiprima@uniss.it
* Correspondence: sergiolozano1391@gmail.com

Abstract: Governments are increasingly committing to significant ecological restoration. However, the impacts of forest restoration on local hydrological services are surprisingly poorly understood. Particularly, limited information is available about the impacts of tree planting on soil infiltration processes and runoff pathways. Thus, we investigated the saturated hydraulic conductivity (K_s) and preferential flow pathways in three land-cover types: (i) Active Restoration, (ii) Degraded Land, and (iii) Reference Forest, with contrasting differences in soil profile and land use history in the municipality of La Jagua de Ibirico, César department, Colombia. We conducted soil sampling, using the Beerkan method to determine K_s values. We also measured vegetation attributes (i.e., canopy cover, vegetation height, diameter at breast height, and total number of trees) and carried out three dye tracer experiments for each study site. The blue dye experiments revealed that near surface matrix infiltration was dominant for Degraded Land, while at the Active Restoration and Reference Forest, this only occurred at local surface depressions. The general infiltration pattern at the three land uses is indicated as being macropore flow with mixed interaction with the matrix and highly affected by the presence of rock fragments. The deeper infiltration patterns occur by preferential flow due to the presence of roots and rock fragments. The mean K_s for the Active Restoration (240 mm h^{-1}) was much higher than the K_s at Degraded Land (40 mm h^{-1}) but still considerably lower than the Reference Forest (324 mm h^{-1}). These results indicate that top soil infiltration capacity and soil physical parameters not only directly regulate the amount of infiltration but also infiltration patterns and runoff processes, leading to lower infiltration and increased excess overland flow for Degraded Land than for other land uses.

Keywords: forest restoration; infiltration capacity; infiltration processes; preferential flow pathways; runoff implications

Citation: Lozano-Baez, S.E.; Domínguez-Haydar, Y.; Zwartendijk, B.W.; Cooper, M.; Tobón, C.; Di Prima, S. Contrasts in Top Soil Infiltration Processes for Degraded vs. Restored Lands. A Case Study at the Perijá Range in Colombia. *Forests* **2021**, *12*, 1716. https://doi.org/10.3390/f12121716

Academic Editor: Daniel McLaughlin

Received: 1 November 2021
Accepted: 1 December 2021
Published: 7 December 2021

1. Introduction

Today, there is no doubt that ecological restoration has great global importance [1,2]. Ambitious international, regional, and national restoration initiatives have emerged to face critical challenges of our time, such as mitigating climate change, conserving biodiversity and recovering hydrological ecosystem services [3,4]. Tree planting is the main driver of the Paris Climate Agreement, of the Bonn challenge, also of the United Nations' Sustainable

Development Goals and the Decade of Ecosystem Restoration (2021–2030) [5]. Thus, there is a critical need to assess the outcomes of forest restoration initiatives [6].

Although the soil is essential for the success of the forest restoration process, soil monitoring is poorly studied [7–9]. The outcomes of forest restoration projects are usually assessed focusing on vegetation attributes [10,11], on the contribution to carbon sequestration or biodiversity conservation [12]. Overall, there are knowledge gaps about the impacts of tree planting on soil ecosystem functions that are essential to sustain ecosystem services for human wellbeing [3,13]. Among these ecosystem functions, water infiltration is important to control soil erosion and runoff, as well as to promote soil moisture content and groundwater recharge [14].

Recent literature reviews have indicated that tree planting in the tropics can improve the water infiltration in degraded soils [3,7,15,16]. Most field studies in forests undergoing restoration [8,17–21] have measured water infiltration on the top-oil focusing on the saturated soil hydraulic conductivity (K_s), only a few scientific works [22–26] have investigated the preferential flow pathways, explaining the water movement through the soil profile. Usually, preferential flow pathways are identified by dye tracer experiments, which have been important in hydrology to understand the water cycle, subsurface flows, and transport processes [27,28].

In the last 50 years, native ecosystems in Colombia have been highly transformed by deforestation and land use change [29,30]. As result, the country has taken steps to restore degraded lands, for instance, Colombia's government recently adopted an ambitious 20-year National Restoration Plan and is actively participating in international restoration initiatives [31]. Nevertheless, restoration projects in Colombia rarely studied soil indicators and the hydrological services provided by tree planting are poorly understood [32].

This investigation aims to broaden the analysis started in a previous work [33], studying a different area within the Perijá Range, Colombia. Specifically, our main objective was to investigate whether the hydrological soil processes are affected by forest restoration, studying the top soil infiltrability in relation to the subsurface percolation pathways. We quantified and compared the K_s and preferential flow pathways of a forest undergoing restoration (hereafter, Active Restoration) with two different land covers, a degraded land (hereafter, Degraded Land), and a secondary old-growth forest (hereafter, Reference Forest). For each land cover type, we examined the possible effects of the topsoil K_s on the theoretical amount of infiltration during rainfall events and runoff processes.

2. Materials and Methods

2.1. Study Area

The study area is located in the sub-basin of the Tucuy River in the Perijá Range, in the municipality of La Jagua de Ibirico, village El Zumbador, César department, Colombia. The area is characterized by steep slopes (>20°); elevation range between 1000 and 1500 m above sea level (Figure 1). The area has a tropical wet–dry climate, Aw according to the Köppen classification; the native vegetation belongs to the Sub-Andean forest; the mean annual temperature is 24 °C, and the average annual precipitation varies between 2200 and 2600 mm per year, with the wettest period from September to November, and the driest period from December to March [34]. The main soil type in the study area is Inceptisols (i.e., Typic Dystropepts) according to USDA Soil Taxonomy [35], which have sandy loam and loam as the dominant soil textures [36].

Over the last 50 years, most of the deforestation in the landscape has been linked to coffee production and livestock grazing [3]. Within the study area, we selected three land cover types of Active Restoration, Degraded Land, and Reference Forest (respectively abbreviated as AR, DL, and RF) to measure soil hydrophysical and vegetation attributes. In each land cover, we established one circular plot, with an area of 160 m^2 each. To avoid large climatological and geological differences, the plots were located at a similar elevation and slope, within a maximum distance of 1.5 km from each other.

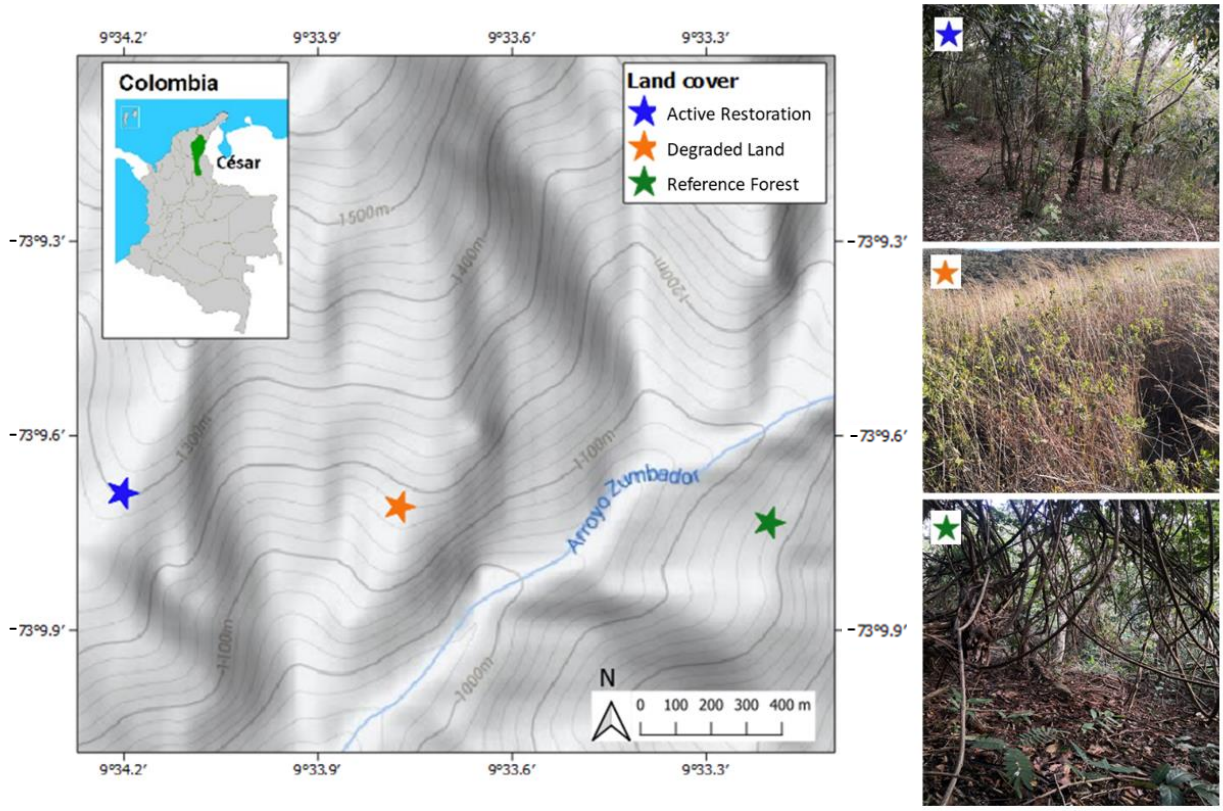

Figure 1. Map of the study area within the Department of Cesar, Colombia, and pictures showing the characteristic vegetation cover of each site.

Land use history for the study sites was reconstructed based on interviews with the local population and aerial photographs. The AR site (9°34′12.26″ N, 73°9′41.33″ W; mean slope: 18°) was initially a forest that was cleared in the middle of the 20th century. After clearing, the site was heavily grazed for more than 30 years. In 2009, native tree plantings were established by forestry offsetting "Vivo Perijá". This program was developed by mining companies, and it has the aim to protect and restore the forests of the Tucuy and Sororia sub-basins [4]. Our measurement in this restoration site represents the effect of 12 years of active restoration on highly degraded soil.

The DL site (9°33′46.83″ N, 73°9′42.62″ W; mean slope: 23°) was cleared first in 1970 by slash and burn. For 40 years the land was used as pasture to raise cattle, in this period the pasture was abandoned many times and later fire was used to clear the area. In 2017 the cattle were excluded, and no fires have been recorded in the last decade. The vegetation cover in the site is dominated by the introduced pasture grass species Jaragua (*Hyperrhenia rufa*), with a mean height of about one meter and isolated native trees and shrub species. Our measurements in this degraded site reflect the influence of an intensive land use history at a highly degraded site after the first four years of the natural regeneration process.

The RF site (9°33′12.18″ N, 73°9′44.05″ W; mean slope: 20°) is a secondary old-growth forest that for the last 40 years has been affected by the selective cutting of trees and fire disturbances coming from adjacent agricultural fields. Additionally, the RF is also affected by the occasional crossing of cattle. Since 2010, the forest was included as an area under conservation in the forestry offsetting "Vivo Perijá", similarly in the region, there are 134 farmers (4666 hectares) who received economic incentives for conserving the forest for 15 years [4]. We used the RF site as a control area to assess reference values for soil properties.

2.2. Field Measurements

2.2.1. Vegetation Sampling

Following our previous investigation [33], we measured the vegetation attributes: (1) canopy cover; (2) vegetation height; (3) diameter at breast height (DBH); and (4) total number of trees. We surveyed all living trees with DBH > 5 cm. We estimated the vegetation height with a 3 m measuring stick, and the remaining height of trees taller than this was estimated visually. We also measured the percentage of canopy cover six times with the mobile application CanopyCapture [37].

2.2.2. Saturated Hydraulic Conductivity

We randomly selected ten sampling points within each study plot for the infiltration measurements. The distance between sampling points was at least 2 m. For measuring the infiltration rates we used the Beerkan method [38]. In total, 30 Beerkan experiments were carried out in February 2021. The values of K_s (mm h^{-1}) were estimated using the Steady version of the Simplified method based on a Beerkan Infiltration run (SSBI method) [39]. The SSBI method was chosen to avoid uncertainties due to a specific shape of the cumulative infiltration [17,40].

For each plot, we collected undisturbed soil cores (100 cm^3) at 0–5 cm depth. We determined the bulk density, BD (g cm^{-3}), and the initial volumetric soil water content θi (cm^3 cm^{-3}). At the end of each infiltration test, a disturbed soil sample was collected to determine the saturated gravimetric water content. The BD was used to calculate the saturated volumetric soil water content, θs (cm^3 cm^{-3}).

2.2.3. Dye Tracer Experiments

For each plot (in each land-cover type), we carried out three dye tracer experiments to investigate the preferential flow pathways formed by roots and soil macroporosity [41]. Following similar investigations [22,42], water with 4 g L^{-1} of Brilliant Blue Dye (FCF C.I. 42090) was sprayed on a 1 m^2 plot for 60 min, with a total volume of 25 mm. The irrigated plots were covered with a plastic sheet and the soil was excavated after 24 h. We excavated three sections per plot, each section was described qualitatively in the field and photographed for subsequent analysis [43] to determine the fraction of stained areas per depth, total stained area per section, amount of stains per section, and the fraction of stains equivalent widths to total stained area (<2 cm, indicating the dominance of preferential flow pathways and low interaction with the matrix; and >20 cm, indication flow with high interaction with the matrix or homogeneous matrix flow). Color adjusting, geometric editing, and soil surface identification of the photos were applied by using the GNU Image Manipulation Program (The GIMP Team. Version 2.10.4; Available online: https://www.gimp.org/ accessed on 9 November 2021).

2.3. Data Analyses

Differences in K_s, BD, θi, θf, canopy cover, vegetation height, DBH, and tracer-experiment characteristics between the respective land-cover types were tested for statistical significance by applying the Kruskal-Wallis analysis. Differences were taken to be significant for values of $p < 0.05$. All vegetation and soil analyses were performed in R software [44], while the tracer experiment analysis was applied using Python V3.7 with Scipy, NumPy, Pandas, Imageio, and Skimage [45–49].

3. Results

Overall, for the vegetation attributes, higher values were observed in the RF. The canopy cover and DBH varied significantly between the AR and RF sites. Only the vegetation height was similar between both land covers. The AR plot evidenced more small trees than the less disturbed forest, moreover, a larger number of trees (34) was counted at the AR site. The vegetation at the DL was dominated by tall grasses with scattered small shrubs and no trees were registered in this site (Table 1).

Table 1. Mean soil properties and vegetation characteristics (±standard deviation) of the forest sites. Different superscript letters denote statistically significant differences between land-cover types ($p < 0.05$). AR, Active Restoration; DL, Degraded land; RF, Reference Forest.

Variable	AR	DL	RF
K_s (mm h^{-1})	240 ± 212 ^{a}	40 ± 34 ^{b}	324 ± 173 ^{a}
BD (g cm^{-3})	1.11 ± 0.16 ^{a}	1.24 ± 0.06 ^{a}	1.18 ± 0.06 ^{a}
θi (cm^3 cm^{-3})	0.08 ± 0.02 ^{a}	0.07 ± 0.02 ^{a}	0.06 ± 0.03 ^{a}
θf (cm^3 cm^{-3})	0.36 ± 0.29 ^{a}	0.27 ± 0.09 ^{a}	0.19 ± 0.04 ^{b}
Canopy cover (%)	50 ± 7 ^{a}	-	80 ± 10 ^{b}
Vegetation height (m)	5 ± 2 ^{a}	-	6 ± 4 ^{a}
Diameter at breast height (cm)	33 ± 17 ^{a}	-	62 ± 48 ^{b}
Total number of trees	34	-	23

The values for the θi were not significantly different between the study plots. The antecedent moisture content, varied between 0.04 to 0.08 cm^3 cm^{-3} and was moderately low for the RF. The θf varied between 0.09 to 0.74 cm^3 cm^{-3} with significantly lower average values for RF than the AR and DL sites (Table 1). The K_s at the soil surface in the study land covers ranged from 7 mm h^{-1} to a maximum of 674 mm h^{-1} (Figure 2). The higher K_s was evidenced in RF (range: 37–674 mm h^{-1}), which was similar to AR (range: 11–655 mm h^{-1}). The K_s was significantly lower for the DL (range: 7–99 mm h^{-1}). The BD ranged from 0.91 to 1.34 g cm^{-3}; there were no significant differences between the plots in terms of BD, although the values were lowest at the AR and highest at the DL site.

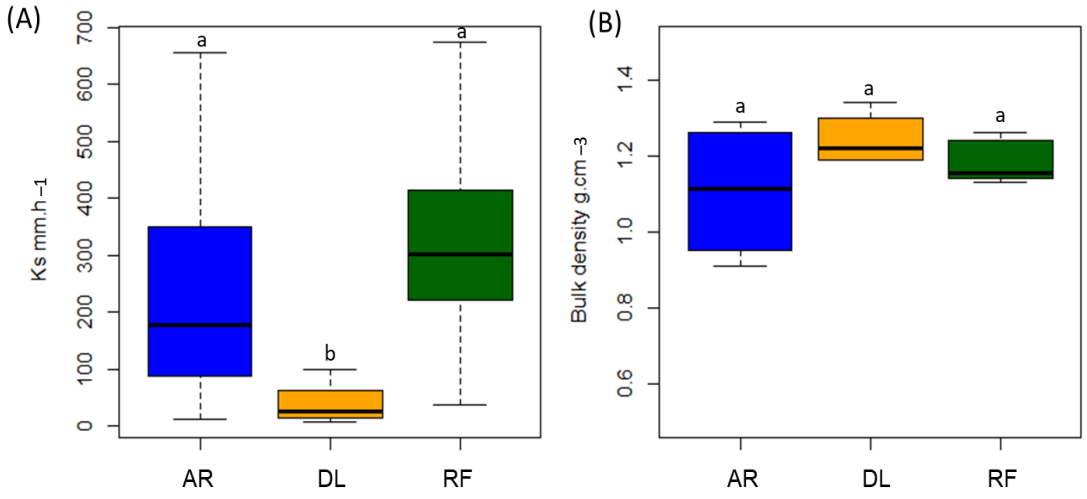

Figure 2. Boxplot of the (**A**) saturated soil hydraulic conductivity (K_s) and (**B**) soil bulk density (g cm^{-3}) for each land cover type. AR, Active Restoration; DL, Degraded Land; RF, Reference Forest. Different letters represent significant differences at $p < 0.05$.

On top of the soil surface a 2, 0.5, and 4 cm layer existed of organic material such as dead leaves and branches for AR, DL, and RF, respectively. The soil layer was very shallow and only a thin (<5 cm) A1 horizon was present at RF. In general, the soil profile below 50 cm could be classified as a mineral horizon containing saprolite and even a transition from the C horizon to bedrock, the amount of cobble to boulders sized rock fragments (from here on referred to as stones [50,51] with sizes varying between 1 and 35 cm) varied a lot; in general, they were very angular and non-spherical, while at the DL the sizes were more homogeneous between 2 and 25 cm and more spherical. In most of the AR and RF sections, at around 30 cm depth, there was an increase in the number of boulders and in some sections weathered rock was found (Figure 3). In some sections, we were not

able to dig deeper than 60 cm below the soil surface due to the amount and size of the rock material.

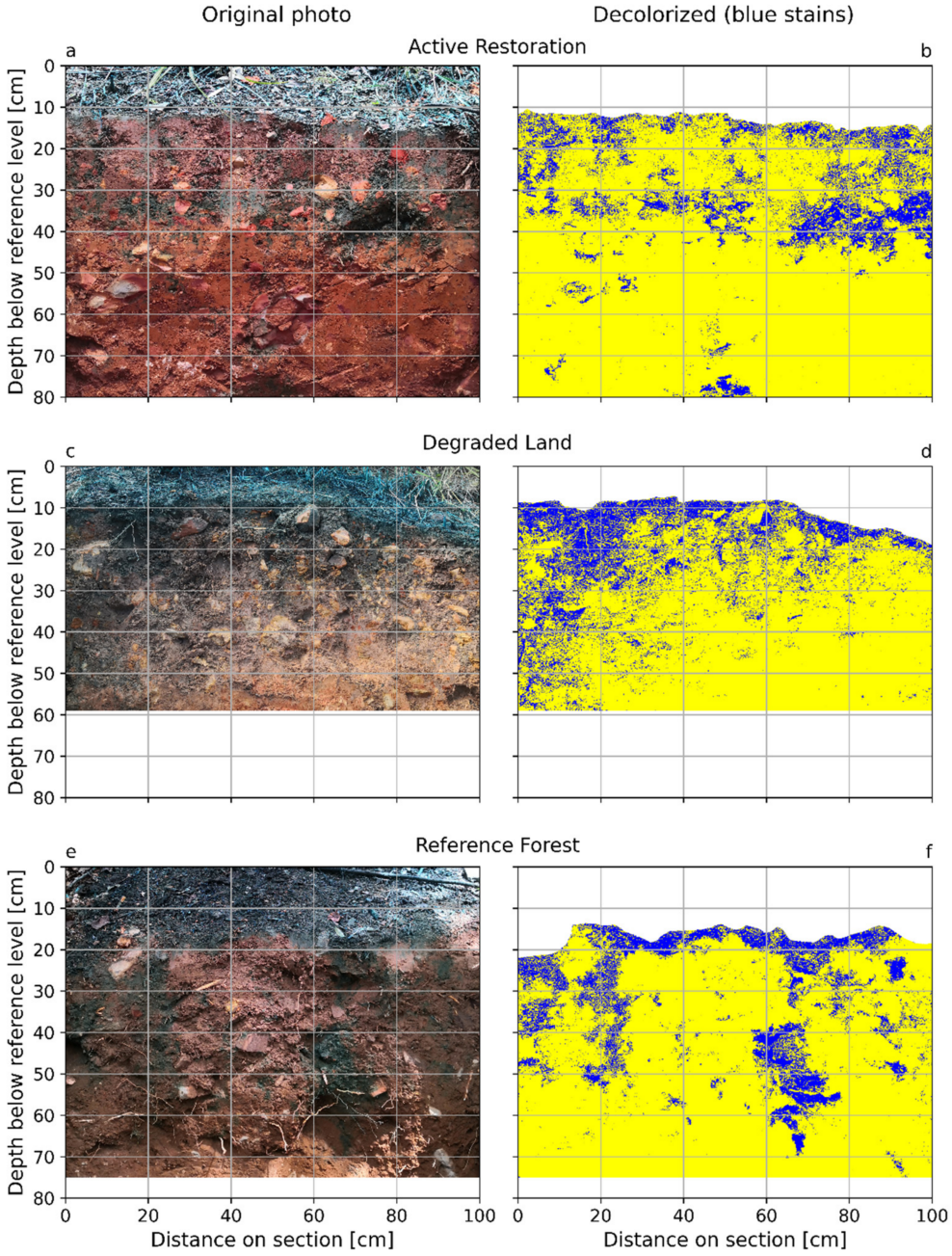

Figure 3. Dye tracer experiments showing the original photo during excavation (**a**,**c**,**e**) and the corrected dye infiltration patterns (**b**,**d**,**f**) for Active Restoration (**a**,**b**), Degraded Land (**c**,**d**), and Reference Forest (**e**,**f**).

In the DL, the top soil infiltration can be qualitatively classified as a heterogeneous matrix flow (top ~5 cm), in AR and RF this pattern was only visible at local surface depressions and is less deep (<4 cm). In the deeper layers, it was visible that more dye occurred along the roots and stones; at DL the deepest observed roots were at ~65 cm depth, while the deepest roots at AR and RF were found at ~95 cm depth. Summarizing, the infiltration types can be qualitatively characterized as macropore flow with mixed (high and low) interaction with the matrix (Figure 3).

The total stained area for the AR sections was the largest (median 1320 cm^2), lower for RF (median 1133 cm^2), and smallest for degraded land (median 927 cm^2) (Table 2).

Differences were only significant between DL and AR. The latter was also the case for the largest stain per section; medians of 837, 233, and 528 cm^2 for respectively AR, DL, and RF, respectively (Table 2). Although no significant differences between the sites were detected for the maximum stained fraction, amount of stains, and fractions of stains (<2 cm and >20 cm), AR showed the largest values for the amount of stains and fraction of stains > 20 cm, indicating the presence of more preferential flow pathways and interactions with the matrix (also being the case for RF) (Table 2 and Figure 4).

Table 2. Median (±standard deviation) values of the results of the blue dye experiments. Different superscript letters denote statistically significant differences between land-cover types ($p < 0.05$). AR, Active restoration; DL, Degraded land; RF, Reference forest.

Variable	AR	DL	RF
Total stained area (cm^2)	1320 ± 707 [a]	927 ± 379 [b]	1133 ± 254 [ab]
Maximum stain area (cm^2)	837 ± 786 [a]	233 ± 223 [b]	528 ± 290 [ab]
Maximum stained fraction (-)	0.63 ± 0.16 [a]	0.53 ± 0.14 [a]	0.58 ± 0.10 [a]
Amount of stains (-)	4744 ± 3166 [a]	2771 ± 2067 [a]	4257 ± 1634 [a]
Fraction of stains <2 cm width to total stained area [%]	18.1 ± 21.6 [a]	18.3 ± 15.5 [a]	17.6 ± 7.0 [a]
Fraction of stains >20 cm width to total stained area [%]	68 ± 31.5 [a]	40.4 ± 20.4 [a]	61.5 ± 20.8 [a]

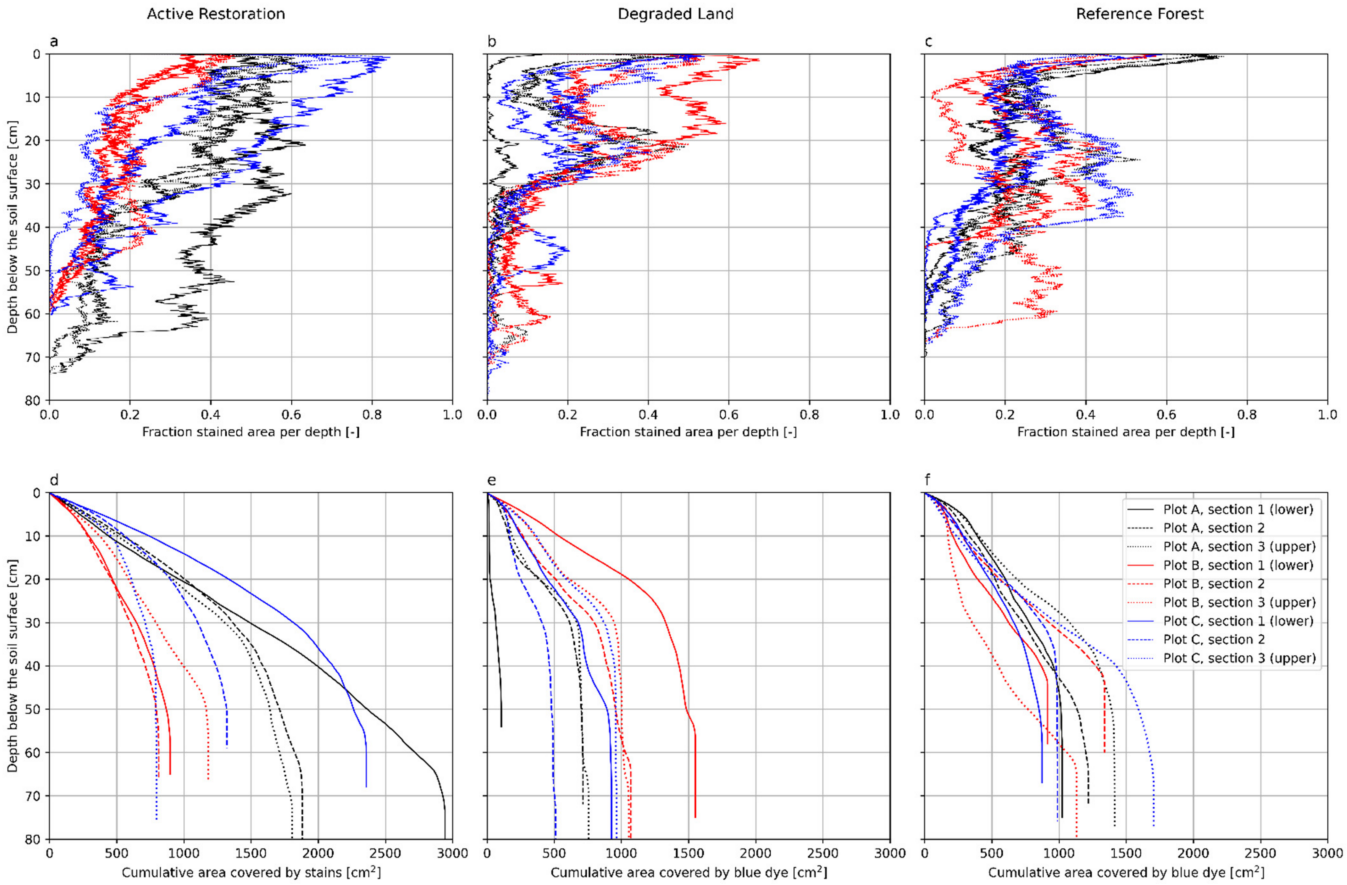

Figure 4. Results of dye tracer experiments showing the nine fractions of stained area per depth (**a**–**c**) and cumulative area covered by stains (**d**–**f**) for Active Restoration (**a**,**d**), Degraded Land (**b**,**e**), and Reference Forest (**c**,**f**). Lines denote sections from down- to upslope (black, grey, red, green, and blue). The continuous lines are from the first plot, dashed lines are from the second plot.

The largest volume of blue dye near the surface was found at RF, varying much more for AR and DL (Figure 4). At RF, the fraction of blue declined rapidly to around 6 cm depth and then increased again in the layer dominated by stones at 15 to 40 cm depth. The fraction of blue below 30 cm depth was lowest for DL and only present along some stones, while at AR, and even more for RF, deeper root penetration leading to larger fractions of blue stain at depths larger than 40 cm was observed (Figures 3 and 4).

4. Discussion

4.1. Space for Time Approach Not Applicable

To ensure the comparison between the study sites, we endeavored to choose plot locations with the least environmental variability. Unfortunately, differences in the soil profile were observed during the field description. Therefore, our study could not use the space-for-time approach. The DL site contained more stones and these stones were located closer to the surface. No previous research or information on erosion and soil texture was available. Based on the information on land use history, we expect that DL endured much more erosion due to the absence of large vegetation, which could have caused a loss of more than 20 cm of soil. Due to the absence of information, we cannot exclude geological differences even though DL is located halfway between RF and AR. Furthermore, no information of the previous soil physical state of AR is available. Therefore, it is not possible to apply the space for time approach.

4.2. Topsoil Properties and Vegetation Characteristics

Not unexpectedly, the highest K_s values were found at the RF, which was also the site with greater values for the vegetation attributes. This result is in line with many tropical studies that observed a high K_s for little disturbed forests [7,19,20,22,33,52,53]. Overall, it is well documented in the literature that a good plant cover can generally prevent surface erosion, and a well-developed tree cover can also reduce shallow landsliding [3,15,54]. The top soil infiltration in the RF could be being influenced by occasional crossing of cattle, which can affect the runoff process. Our mean K_s in the RF (324 mm h^{-1}) site was lower than the mean reported value of 469 mm h^{-1} in a previous study [33] for a secondary old-growth forest that was more than 50-years-old. In that study, K_s was also measured in a forest with 15 years of natural regeneration, showing a mean value of 244 mm h^{-1}, interestingly this value was similar with the mean K_s in the AR (240 mm h^{-1}), which can be interpreted as a recovery after a certain degree of degradation [55]. Both, the active and the natural regenerated forests in our study did not reach the K_s reported at the shade-grown coffee (mean 322 mm h^{-1}) site [33]. Planting trees in coffee plantations is a highly recommended practice to reduce soil erosion and increase the infiltration capacity [56,57]. For the DL, the mean K_s (40 mm h^{-1}) was higher than the pasture (12 mm h^{-1}) sampled previously. This difference can be explained by the intensity of land use and the more recent trampling of cattle in the pasture [17].

4.3. Infiltration Characteristics and Implications for Runoff Processes

Due to the absence of variations in flow types and stained parameters between sites and sections, quantitative flow type determination as in Weiler et al. [43] was not applicable for our sites. Qualitative observations of the infiltration patterns (Figure 3) and stained parameters indicated; heterogeneous matrix flow and fingering near the surface while percolation patterns were dominated by macropore flow with mixed (high and low) interaction at deeper layers around stones and roots. As in Zwartendijk et al. [22], fewer preferential flow pathways existed in DL than to RF, but when they occurred, the water was able to move deeper due to the lower interaction with the matrix. Comparable research as in Collof et al. [58], Hanson et al. [59] and Zwartendijk et al. [22] indicated that macropores in degraded lands were filled by fine soil particles and so blocked macropore flow. For our case, this was only true for the top layer blocking water to infiltrate to the deeper layers, while deeper flow patterns were affected by preferential flow around stones and to

a minor extent roots, which did not show significant differences between DL and the other land uses.

Future research carried out at the sub-basin of the Tucuy River should seek to address the role that tree planting plays on ecohydrological processes and water dynamics also at a larger scale (e.g., hillslope scale and sub-basin scale). For this aim, geophysical techniques, such as ground-penetrating radar (GPR), may be adopted for noninvasive monitoring of the temporal and spatial distribution of water flow and preferential low pathways detection [60,61].

Together with the steep topography (>15 degrees) and the local depressions, the topsoil K_s dominantly affects the volume of water infiltration during rainfall events and groundwater recharge and can also be affected by the previous wetness of the soils, the rainfall amount, duration, and intensities [23,62–64]. To have a proper understanding of the actual infiltration and runoff processes, it is important to understand the precipitation characteristics. The nearest daily rainfall is measured approximately 60 km away from the research area at an elevation of 900 m ASL, with annual rainfall between 930 and 3500 mm per year (median 2030 mm per year), 24% of rainy days (>1 mm rainfall), median daily precipitation of 12 mm, and maximum of 160 mm (Figure S1), which matches the annual precipitation between 2200 and 2600 mm per year as mentioned in [34]. At higher elevations, at 480 km from our study area [65], measured precipitation occurs at altitudes between 1550 and 2300 m, identifying wetter and less seasonal conditions at higher elevations, indicating a positive relation between elevation and fog or rainfall persistence. Annual rainfall for the two rainfall gauges at the low elevation sites (3900 mm) were similar but considerably lower than those observed at the high elevation station (4700 mm). The same study mentioned that seasonally mean daily rainfall at the lower elevations were 15 mm during the wet and 3 mm during the dry season. Further, 25 km away from the sites of Ramírez et al. [65] at an elevation of 1550 m ASL, Peralta and Ataroff [66] measured 3670 mm annual rainfall.

To estimate the runoff processes during a rainfall event, we selected comparable research [14,19,23,67,68], although at lower elevation and lower annual precipitation, we expect 5-min rainfall intensities larger than 75 mm h^{-1}, 10-min larger than 45 mm h^{-1}, and even hourly rainfall exceeding 20 mm h^{-1} (Table S1). Comparing these intensities to the measured top soil infiltration capacities on the steep slopes, this means that the infiltration excess overland flow (IOF) will be the dominant runoff mechanism at DL (mean K_s of 40 mm h^{-1}, standard deviation 34 mm h^{-1}). The variation in K_s for AR indicates that locally IOF will occur, but this flow may infiltrate at locations where the values are much higher (mean K_s of 240 mm h^{-1}, standard deviation 212), and it is unlikely that IOF will occur at RF (mean K_s of 324 mm h^{-1}, standard deviation 173 mm h^{-1}). The latter is in line with research elsewhere [15,16,23,24]. To have a better understanding of hillslope scales it is recommended to apply larger scale measurements of overland flow, subsurface processes, and precipitation measurements.

5. Conclusions

Our study combined vegetation sampling, K_s measurements, and dye tracer experiments in three land-cover types: AR, DL, and RF, with contrasting differences in soil profile and land use history. Compared with previous research, our measurements indicated no significant differences for top soil infiltration capacity between Active Restoration and Reference Forest and significant differences between these land uses and Degraded Land. Although bulk density values were lowest at the AR and highest at the DL site, there were no significant differences between the plots. The blue dye experiments revealed that near surface matrix infiltration was dominant at DL but less abundant at AR and RF. The general flow pattern was identified as macropore flow with varying interactions with the soil matrix. The preferential flow at 25 cm depth was mainly affected by the presence of a layer dominated by stones with high interaction with the soil matrix. Although visually preferential flow in deeper layers was dominated by roots (more in RF, less in AR,

and absent in DL) and stones, no significant differences were determined for maximum stained fraction, number of stains, and fractions of width for the three sites. The total and maximum stain area was largest for AR and differed significantly from DL.

The significant differences in top soil K_s for DL (mean 40 mm h^{-1}) compared to AR and RF (mean values of 240 and 324 mm h^{-1}, respectively) indicated that top soil infiltration capacity and soil physical parameters not only directly regulate the amount of infiltration but also infiltration patterns and runoff processes, leading to more infiltration excess overland flow for Degraded Land than for other land uses. We highly recommend that geology and the presence of stones within the subsoil must not be omitted while studying these processes and the hydrogeological effects of land use changes.

Supplementary Materials: The following are available online at https://www.mdpi.com/article/10.3390/f12121716/s1, Figure S1: Daily precipitation time series for the station "La Jagua de Ibirico" in Colombia. Table S1: Published studies showing the characteristic of rainfall events.

Author Contributions: S.E.L.-B. carried out the data collection. S.E.L.-B. and B.W.Z. wrote the initial draft. Y.D.-H. participated in the design of the study. B.W.Z. analyzed the data and made great contributions to writing the manuscript. M.C., C.T. and S.D.P. revised, discussed, modified, and supplemented the ideas for the final draft. All authors have read and agreed to the published version of the manuscript.

Funding: This research was funded by the Colombian Ministry of Science (Grant No. 848) and "Vicerrectoría de Investigaciones, Extensión y Proyección Social" of Universidad del Atlántico. Bob Zwartendijk acknowledges financial support from the Dutch Research Council (NWO) "Doctoral Grand for Teachers" (023.016.033).

Institutional Review Board Statement: Not applicable.

Informed Consent Statement: Not applicable.

Acknowledgments: We thank Jhon Jairo Carvajal Pérez, Eduver Abril Navarro, Hubercito Garcia, and Jadier Quintero Díaz for the help during the field work.

Conflicts of Interest: The authors declare no conflict of interest.

References

1. Chazdon, R.L.; Brancalion, P.H.S.; Lamb, D.; Laestadius, L.; Calmon, M.; Kumar, C. A Policy-Driven Knowledge Agenda for Global Forest and Landscape Restoration: A Policy-Driven Agenda for Restoration. *Conserv. Lett.* **2017**, *10*, 125–132. [CrossRef]
2. Brancalion, P.H.S.; Niamir, A.; Broadbent, E.; Crouzeilles, R.; Barros, F.S.M.; Zambrano, A.M.A.; Baccini, A.; Aronson, J.; Goetz, S.; Reid, J.L.; et al. Global restoration opportunities in tropical rainforest landscapes. *Sci. Adv.* **2019**, *5*, eaav3223. [CrossRef] [PubMed]
3. Filoso, S.; Bezerra, M.O.; Weiss, K.C.B.; Palmer, M.A. Impacts of forest restoration on water yield: A systematic review. *PLoS ONE* **2017**, *12*, e0183210. [CrossRef] [PubMed]
4. Strassburg, B.B.N.; Iribarrem, A.; Beyer, H.L.; Cordeiro, C.L.; Crouzeilles, R.; Jakovac, C.C.; Junqueira, A.B.; Lacerda, E.; Latawiec, A.E.; Balmford, A.; et al. Global priority areas for ecosystem restoration. *Nature* **2020**, *586*, 724–729. [CrossRef] [PubMed]
5. Brancalion, P.H.S.; Holl, K.D. Guidance for successful tree planting initiatives. *J. Appl. Ecol.* **2020**, *57*, 2349–2361. [CrossRef]
6. Gatica-Saavedra, P.; Echeverría, C.; Nelson, C.R. Ecological indicators for assessing ecological success of forest restoration: A world review: Indicators for Forest Restoration. *Restor. Ecol.* **2017**, *25*, 850–857. [CrossRef]
7. Lozano-Baez, S.E.; Cooper, M.; Meli, P.; Ferraz, S.F.; Rodrigues, R.R.; Sauer, T.J. Land restoration by tree planting in the tropics and subtropics improves soil infiltration, but some critical gaps still hinder conclusive results. *For. Ecol. Manag.* **2019**, *444*, 89–95. [CrossRef]
8. Pereira, N.A.; Di Prima, S.; Bovi, R.C.; Da Silva, L.F.S.; De Godoy, G.; Naves, R.P.; Cooper, M. Does the Process of Passive Forest Restoration Affect the Hydrophysical Attributes of the Soil Superficial Horizon? *Water* **2020**, *12*, 1689. [CrossRef]
9. Sun, D.; Yang, H.; Guan, D.; Yang, M.; Wu, J.; Yuan, F.; Jin, C.; Wang, A.; Zhang, Y. The effects of land use change on soil infiltration capacity in China: A meta-analysis. *Sci. Total Environ.* **2018**, *626*, 1394–1401. [CrossRef]
10. Kardol, P.; Wardle, D. How understanding aboveground–belowground linkages can assist restoration ecology. *Trends Ecol. Evol.* **2010**, *25*, 670–679. [CrossRef]
11. Ohsowski, B.M.; Klironomos, J.N.; Dunfield, K.E.; Hart, M.M. The potential of soil amendments for restoring severely disturbed grasslands. *Appl. Soil Ecol.* **2012**, *60*, 77–83. [CrossRef]
12. Mukul, S.A.; Herbohn, J.; Firn, J. Co-benefits of biodiversity and carbon sequestration from regenerating secondary forests in the Philippine uplands: Implications for forest landscape restoration. *Biotropica* **2016**, *48*, 882–889. [CrossRef]

13. Barral, M.P.; Benayas, J.M.R.; Meli, P.; Maceira, N.O. Quantifying the impacts of ecological restoration on biodiversity and ecosystem services in agroecosystems: A global meta-analysis. *Agric. Ecosyst. Environ.* **2015**, *202*, 223–231. [CrossRef]
14. Ziegler, A.D.; Giambelluca, T.W.; Tran, L.T.; Vana, T.T.; Nullet, M.A.; Fox, J.; Vien, T.D.; Pinthong, J.; Maxwell, J.; Evett, S. Hydrological consequences of landscape fragmentation in mountainous northern Vietnam: Evidence of accelerated overland flow generation. *J. Hydrol.* **2004**, *287*, 124–146. [CrossRef]
15. Ilstedt, U.; Malmer, A.; Verbeeten, E.; Murdiyarso, D. The effect of afforestation on water infiltration in the tropics: A systematic review and meta-analysis. *For. Ecol. Manag.* **2007**, *251*, 45–51. [CrossRef]
16. Bonnesoeur, V.; Locatelli, B.; Guariguata, M.R.; Ochoa-Tocachi, B.F.; Vanacker, V.; Mao, Z.; Stokes, A.; Mathez-Stiefel, S.-L. Impacts of forests and forestation on hydrological services in the Andes: A systematic review. *For. Ecol. Manag.* **2019**, *433*, 569–584. [CrossRef]
17. Lozano-Baez, S.E.; Cooper, M.; Ferraz, S.F.B.; Rodrigues, R.R.; Pirastru, M.; Di Prima, S. Previous Land Use Affects the Recovery of Soil Hydraulic Properties after Forest Restoration. *Water* **2018**, *10*, 453. [CrossRef]
18. Lozano-Baez, S.E.; Cooper, M.; Ferraz, S.F.D.B.; Rodrigues, R.R.; Castellini, M.; Di Prima, S. Recovery of Soil Hydraulic Properties for Assisted Passive and Active Restoration: Assessing Historical Land Use and Forest Structure. *Water* **2019**, *11*, 86. [CrossRef]
19. Zimmermann, B.; Elsenbeer, H.; De Moraes, J.M. The influence of land-use changes on soil hydraulic properties: Implications for runoff generation. *For. Ecol. Manag.* **2006**, *222*, 29–38. [CrossRef]
20. Bonell, M.; Purandara, B.; Venkatesh, B.; Krishnaswamy, J.; Acharya, H.; Singh, U.; Jayakumar, R.; Chappell, N. The impact of forest use and reforestation on soil hydraulic conductivity in the Western Ghats of India: Implications for surface and sub-surface hydrology. *J. Hydrol.* **2010**, *391*, 47–62. [CrossRef]
21. Leite, P.A.; De Souza, E.S.; Dos Santos, E.S.; Gomes, R.J.; Cantalice, J.R.; Wilcox, B. The influence of forest regrowth on soil hydraulic properties and erosion in a semiarid region of Brazil. *Ecohydrology* **2017**, *11*, e1910. [CrossRef]
22. Zwartendijk, B.; van Meerveld, H.; Ghimire, C.; Bruijnzeel, L.; Ravelona, M.; Jones, J. Rebuilding soil hydrological functioning after swidden agriculture in eastern Madagascar. *Agric. Ecosyst. Environ.* **2017**, *239*, 101–111. [CrossRef]
23. Zwartendijk, B.; van Meerveld, H.; Ghimire, C.; Ravelona, M.; Lahitiana, J.; Bruijnzeel, L. Soil water- and overland flow dynamics in a tropical catchment subject to long-term slash-and-burn agriculture. *J. Hydrol.* **2020**, *582*, 124287. [CrossRef]
24. van Meerveld, H.J.; Jones, J.P.G.; Ghimire, C.P.; Zwartendijk, B.W.; Lahitiana, J.; Ravelona, M.; Mulligan, M. Forest regeneration can positively contribute to local hydrological ecosystem services: Implications for forest landscape restoration. *J. Appl. Ecol.* **2021**, *58*, 755–765. [CrossRef]
25. Saputra, D.D.; Sari, R.R.; Hairiah, K.; Roshetko, J.M.; Suprayogo, D.; Van Noordwijk, M. Can cocoa agroforestry restore degraded soil structure following conversion from forest to agricultural use? *Agrofor. Syst.* **2020**, *94*, 2261–2276. [CrossRef]
26. Jačka, L.; Walmsley, A.; Kovář, M.; Frouz, J. Effects of different tree species on infiltration and preferential flow in soils developing at a clayey spoil heap. *Geoderma* **2021**, *403*, 115372. [CrossRef]
27. Flury, M.; Wai, N.N. Dyes as tracers for vadose zone hydrology. *Rev. Geophys.* **2003**, *41*, 1002. [CrossRef]
28. Kodešová, R.; Němeček, K.; Kodeš, V.; Žigová, A. Using Dye Tracer for Visualization of Preferential Flow at Macro- and Microscales. *Vadose Zone J.* **2012**, *11*, vzj2011.0088. [CrossRef]
29. Etter, A.; Andrade, A.; Nelson, C.R.; Cortés, J.; Saavedra, K. Assessing restoration priorities for high-risk ecosystems: An application of the IUCN Red List of Ecosystems. *Land Use Policy* **2020**, *99*, 104874. [CrossRef]
30. Etter, A.; McAlpine, C.; Possingham, H. Historical Patterns and Drivers of Landscape Change in Colombia Since 1500: A Regionalized Spatial Approach. *Ann. Assoc. Am. Geogr.* **2008**, *98*, 2–23. [CrossRef]
31. Aguilar, M.; Sierra, J.; Ramirez, W.; Vargas, O.; Calle, Z.; Vargas, W.; Murcia, C.; Aronson, J.; Cataño, J.I.B. Toward a post-conflict Colombia: Restoring to the future. *Restor. Ecol.* **2015**, *23*, 4–6. [CrossRef]
32. Lozano-Baez, S.E.; Domínguez-Haydar, Y.; Meli, P.; Meerveld, I.; Vásquez, K.V.; Castellini, M. Key gaps in soil monitoring during forest restoration in Colombia. *Restor. Ecol.* **2021**, *29*, 13391. [CrossRef]
33. Lozano-Baez, S.; Domínguez-Haydar, Y.; Di Prima, S.; Cooper, M.; Castellini, M. Shade-Grown Coffee in Colombia Benefits Soil Hydraulic Conductivity. *Sustainability* **2021**, *13*, 7768. [CrossRef]
34. Rangel-Ch, J.O. Integrated climate of the Perijá massif, Colombia. In *Colombia Diversidad Biótica XVIII: Biodiversidad y Territorio de la Serranía de Perijá (Cesar-Colombia)*; Universidad Nacional de Colombia: Bogotá, Colombia, 2019; pp. 92–128.
35. USDA-Natural Resources Conservation Service. Soil Survey Staff. In *Keys to Soil Taxonomy*, 12th ed.; USDA-Natural Resources Conservation Service: Washington, DC, USA, 2014.
36. Rangel-Ch, J.O.; Carvajal-Cogollo, J.E.; Arellano-P, H. Suelos de la Serranía de Perijá. In *Colombia Diversidad Biótica XVIII: Media y Baja Montaña de la Serranía de Perijá*; Rangel-Ch, J.O., Ed.; Universidad Nacional de Colombia: Bogotá, Colombia, 2010; pp. 51–72.
37. Nikhil, P. *Canopy Capture a Smarter Way to Measure Canopy Cover*. Available online: https://nikp29.github.io/CanopyCapture/ (accessed on 9 July 2021).
38. Lassabatère, L.; Angulo-Jaramillo, R.; Ugalde, J.M.S.; Cuenca, R.; Braud, I.; Haverkamp, R. Beerkan Estimation of Soil Transfer Parameters through Infiltration Experiments-BEST. *Soil Sci. Soc. Am. J.* **2006**, *70*, 521–532. [CrossRef]
39. Bagarello, V.; Di Prima, S.; Iovino, M. Estimating saturated soil hydraulic conductivity by the near steady-state phase of a Beerkan infiltration test. *Geoderma* **2017**, *303*, 70–77. [CrossRef]
40. Di Prima, S.; Concialdi, P.; Lassabatere, L.; Angulo-Jaramillo, R.; Pirastru, M.; Cerdà, A.; Keesstra, S. Laboratory testing of Beerkan infiltration experiments for assessing the role of soil sealing on water infiltration. *Catena* **2018**, *167*, 373–384. [CrossRef]

41. Beven, K.; Germann, P. Macropores and water flow in soils. *Water Resour. Res.* **1982**, *18*, 1311–1325. [CrossRef]
42. Ghimire, C.P.; Zwartendijk, B.W.; Pde, F.; Bruijnzeel, L.A. Changes in Soil Hydraulic Conductivity and Preferential Flow Pathways after Assisted Forest Restoration on Degraded Land in the Khasi Hills (Meghalaya, NE India). In Proceedings of the EGU General Assembly 2021, online, 19–30 April 2021. EGU21-6559. [CrossRef]
43. Weiler, M.; Flühler, H. Inferring flow types from dye patterns in macroporous soils. *Geoderma* **2004**, *120*, 137–153. [CrossRef]
44. R Core Team. *R: A Language and Environment for Statistical Computing*; R Foundation for Statistical Computing: Viena, Austria, 2021.
45. Virtanen, P.; Gommers, R.; Oliphant, T.E.; Haberland, M.; Reddy, T.; Cournapeau, D.; Burovski, E.; Peterson, P.; Weckesser, W.; Bright, J.; et al. SciPy 1.0: Fundamental algorithms for scientific computing in Python. *Nat. Methods* **2020**, *17*, 261–272. [CrossRef]
46. Harris, C.R.; Millman, K.J.; van der Walt, S.J.; Gommers, R.; Virtanen, P.; Cournapeau, D.; Wieser, E.; Taylor, J.; Berg, S.; Smith, N.J.; et al. Array programming with NumPy. *Nature* **2020**, *585*, 357–362. [CrossRef]
47. Hunter, J.D. Matplotlib: A 2D Graphics Environment. *Comput. Sci. Eng.* **2007**, *9*, 90–95. [CrossRef]
48. Van Der Walt, S.; Schönberger, J.L.; Nunez-Iglesias, J.; Boulogne, F.; Warner, J.; Yager, N.; Gouillart, E.; Yu, T. Scikit-Image: Image processing in Python. *PeerJ* **2014**, *2*, e453. [CrossRef]
49. Silvester, S.; Tanbakuchi, A.; Müller, P.; Nunez-Iglesias, J.; Harfouche, M.; Klein, A.; McCormick, M.; Irradiation, O.; Rai, A.; Ladegaard, A.; et al. *Imageio/Imageio*; v2.13.1 (v2.13.1); Zenodo: Genève, Switzerland, 2021. [CrossRef]
50. Udden, J.A. Mechanical composition of clastic sediments. *GSA Bull.* **1914**, *25*, 655–744. [CrossRef]
51. FAO. *Guidelines for Soil Description*; Food and Agriculture Organization of the United Nations: Rome, Italy, 2006.
52. Zimmermann, B.; Papritz, A.; Elsenbeer, H. Asymmetric response to disturbance and recovery: Changes of soil permeability under forest–pasture–forest transitions. *Geoderma* **2010**, *159*, 209–215. [CrossRef]
53. Ghimire, C.P.; Bruijnzeel, L.A.; Bonell, M.; Coles, N.; Lubczynski, M.W.; Gilmour, D.A. The effects of sustained forest use on hillslope soil hydraulic conductivity in the Middle Mountains of Central Nepal: Sustained Forest Use and Soil Hydraulic Conductivity. *Ecohydrology* **2014**, *7*, 478–495. [CrossRef]
54. Ilstedt, U.; Tobella, A.B.; Bazié, H.R.; Bayala, J.; Verbeeten, E.; Nyberg, G.; Sanou, J.; Benegas, L.; Murdiyarso, D.; Laudon, H.; et al. Intermediate tree cover can maximize groundwater recharge in the seasonally dry tropics. *Sci. Rep.* **2016**, *6*, 21930. [CrossRef]
55. García-Leoz, V.; Villegas, J.C.; Suescún, D.; Flórez, C.P.; Merino-Martín, L.; Betancur, T.; León, J.D. Land cover effects on water balance partitioning in the Colombian Andes: Improved water availability in early stages of natural vegetation recovery. *Reg. Environ. Chang.* **2018**, *18*, 1117–1129. [CrossRef]
56. Ibanez, M.; Blackman, A. Is Eco-Certification a Win–Win for Developing Country Agriculture? Organic Coffee Certification in Colombia. *World Dev.* **2016**, *82*, 14–27. [CrossRef]
57. Benegas, L.; Ilstedt, U.; Roupsard, O.; Jones, J.; Malmer, A. Effects of trees on infiltrability and preferential flow in two contrasting agroecosystems in Central America. *Agric. Ecosyst. Environ.* **2014**, *183*, 185–196. [CrossRef]
58. Colloff, M.J.; Pullen, K.R.; Cunningham, S. Restoration of an Ecosystem Function to Revegetation Communities: The Role of Invertebrate Macropores in Enhancing Soil Water Infiltration. *Restor. Ecol.* **2010**, *18*, 65–72. [CrossRef]
59. Hanson, D.L.; Steenhuis, T.S.; Walter, M.F.; Boll, J. Effects of soil degradation and management practices on the surface water dynamics in the Talgua River Watershed in Honduras. *Land Degrad. Dev.* **2004**, *15*, 367–381. [CrossRef]
60. Di Prima, S.; Winiarski, T.; Angulo-Jaramillo, R.; Stewart, R.D.; Castellini, M.; Najm, M.R.A.; Ventrella, D.; Pirastru, M.; Giadrossich, F.; Capello, G.; et al. Detecting infiltrated water and preferential flow pathways through time-lapse ground-penetrating radar surveys. *Sci. Total Environ.* **2020**, *726*, 138511. [CrossRef] [PubMed]
61. Di Prima, S.; Giannini, V.; Roder, L.R.; Giadrossich, F.; Lassabatere, L.; Stewart, R.D.; Najm, M.R.A.; Longo, V.; Campus, S.; Winiarski, T.; et al. Coupling time-lapse ground penetrating radar surveys and infiltration experiments to characterize two types of non-uniform flow. *Sci. Total Environ.* **2022**, *806*, 150410. [CrossRef] [PubMed]
62. Xu, C.; Yang, Z.; Qian, W.; Chen, S.; Liu, X.; Lin, W.; Xiong, D.; Jiang, M.; Chang, C.; Huang, J.; et al. Runoff and soil erosion responses to rainfall and vegetation cover under various afforestation management regimes in subtropical montane forest. *Land Degrad. Dev.* **2019**, *30*, 1711–1724. [CrossRef]
63. Western, A.W.; Grayson, R.B.; Bloschl, G.; Willgoose, G.R.; McMahon, T.A. Observed spatial organization of soil moisture and its relation to terrain indices. *Water Resour. Res.* **1999**, *35*, 797–810. [CrossRef]
64. Peng, Z.; Hu, H.; Tian, F.; Tie, Q.; Zhao, S. Impacts of Rainfall Features and Antecedent Soil Moisture on Occurrence of Preferential Flow: A Study at Hillslopes Using High-Frequency Monitoring. *Hydrol. Earth Syst. Sci.* **2016**, 1–12. [CrossRef]
65. Ramírez, B.H.; Teuling, A.J.; Ganzeveld, L.; Hegger, Z.; Leemans, R. Tropical Montane Cloud Forests: Hydrometeorological variability in three neighbouring catchments with different forest cover. *J. Hydrol.* **2017**, *552*, 151–167. [CrossRef]
66. Peralta, H.; Ataroff, M. *Hídrica en la Selva Nublada de la Cuenca Alta del rio Cusiana y un Pastizal de Reemplazo, Cordillera Oriental, Colombia*; Ataroff, M., Silva, J.F., Eds.; ICAE, Universidad de los Andes: Mérida, Venezuela, 2005; pp. 31–36.
67. Zimmermann, B.; Elsenbeer, H. The near-surface hydrological consequences of disturbance and recovery: A simulation study. *J. Hydrol.* **2009**, *364*, 115–127. [CrossRef]
68. Ziegler, A.D.; Negishi, J.N.; Sidle, R.C.; Noguchi, S.; Nik, A.R. Impacts of logging disturbance on hillslope saturated hydraulic conductivity in a tropical forest in Peninsular Malaysia. *Catena* **2006**, *67*, 89–104. [CrossRef]